Direct Triblock-Copolymer-Templating Synthesis of Highly Ordered Fluorinated Mesoporous Carbon[†]

Ying Wan,*,[‡] Xufang Qian,[‡] Nengqin Jia,[‡] Zhiyong Wang,[‡] Hexing Li,[‡] and Dongyuan Zhao[§]

Department of Chemistry, Shanghai Normal University, Shanghai 200234, P. R. China, and Department of Chemistry, Shanghai Key Laboratory of Molecular Catalysis and Innovative Materials, Fudan University, Shanghai 200433, P. R. China

Received June 4, 2007. Revised Manuscript Received August 23, 2007

Highly ordered mesoporous carbons have been synthesized from a direct triblock-copolymer-templating process of organic–organic self-assembly. The organic precursors are phenol, formaldehyde, and a functional monomer of *p*-fluorophenol, and the organic structure directing agent is triblock copolymer Pluronic F127. Characterization using X-ray diffraction (XRD), transmission electron microscopy (TEM), Raman, Fourier transform infrared (FTIR), and nitrogen adsorption techniques reveals that the fluorinated carbons possess highly ordered mesostructures, high surface areas (693–998 m^2/g), large pore sizes (3.0–4.4 nm), large pore volumes (0.43–0.70 cm^3/g), and C–F covalent bonds after high-temperature carbonization at 900 °C. Various mesostructures such as 2D hexagonal and 3D body-centered cubic structures can be synthesized by simply tuning the ratios of *p*-fluorophenol/phenol or phenol/triblock copolymer. The fluorinated mesoporous carbon modified glassy carbon (GC) electrode exhibits higher electron transfer rate than both pure mesoporous carbon FDU-15 modified and bare GC electrodes. This result further indicates the fluorination of mesoporous carbons and the potential for fluorinated mesoporous carbons in electrocatalytic reactions.

1. Introduction

Carbon-based materials are of great interest owing to the advantages of low cost, large surface area, high stability, controllable pore texture, and tunable surface chemistry. The modification of the structural and chemical properties of carbon materials, in particular fluorination, has long been studied to widen their applications in electric conductors, primary and secondary batteries, electromagnetic materials, and aerospace technology.[1–4] Traditional modification methods mainly include the following: (1) oxidation with nitric acid or ozone, which produces oxygenated functionalities; (2) grafting of moieties via aryl diazonium or azomethine ylides; (3) modification with carbenes or nitrenes; (4) reduction with lithium compounds; and (5) vapor deposition and reaction.[3–10] The frequently used route is vapor deposition, such as sweeping with fluorine gas.[9,11–13] However, the functionalization of carbon is encountered with the problems of poor controllability due to the inert surface.

Confined-space effects inside the mesostructured channels would certainly modify the unique physical and chemical properties of carbons, which have inspired chemists and material scientists to create uniform mesoporous carbons. Ryoo and co-workers first fabricated ordered mesoporous carbon by a nanocasting method.[14] Carbon precursors are first introduced into the channels of the mesoporous silicates through either a solution-phase or a vapor-phase reaction with the inorganic hosts and transformed to carbons through carbonization. After the removal of the silica hard templates, mesoporous carbon nanowire, nanorod, or nanotube arrays replicate the ordered mesostructures of silicates.[14–26] When the carbon source consists of functional groups, for example, ethylenediamine, mesoporous carbon replica contains heteroatoms such as N.[27] Only a few studies have been carried out on the functionalization mainly due to the loss of moieties during the high-temperature carbonization.[28–33] Compared with mesoporous silicates which have reactive hydroxyls on the surface, mesoporous carbons lack active groups. The

---

[†] Part of the "Templated Materials Special Issue".

* To whom correspondence should be addressed. Tel: 86-21-6432-2642. Fax: 86-21-6432-2272. E-mail: ywan@shnu.edu.cn.

[‡] Shanghai Normal University.

[§] Fudan University.

(1) Plank, N. O. V.; Forrest, G. A.; Cheung, R.; Alexander, A. J. *J. Phys. Chem. B* **2005**, *109*, 22096.

(2) Nakajima, T.; Li, J. L.; Naga, K.; Yoneshima, K.; Nakai, T.; Ohzawa, Y. *J. Power Sources* **2004**, *133*, 243.

(3) Bahr, J. L.; Yang, J. P.; Kosynkin, D. V.; Bronikowski, M. J.; Smalley, R. E.; Tour, J. M. *J. Am. Chem. Soc.* **2001**, *123*, 6536.

(4) Bahr, J. L.; Tour, J. M. *Chem. Mater.* **2001**, *13*, 3823.

(5) Dyke, C. A.; Tour, J. M. *J. Am. Chem. Soc.* **2003**, *125*, 1156.

(6) Georgakilas, V.; Voulgaris, D.; Vazquez, E.; Prato, M.; Guldi, D. M.; Kukovecz, A.; Kuzmany, H. *J. Am. Chem. Soc.* **2002**, *124*, 14318.

(7) Chen, J.; Hamon, M. A.; Hu, H.; Chen, Y. S.; Rao, A. M.; Eklund, P. C.; Haddon, R. C. *Science* **1998**, *282*, 95.

(8) Mickelson, E. T.; Chiang, I. W.; Zimmerman, J. L.; Boul, P. J.; Lozano, J.; Liu, J.; Smalley, R. E.; Hauge, R. H.; Margrave, J. L. *J. Phys. Chem. B* **1999**, *103*, 4318.

(9) Li, Z. J.; Del Cul, G. D.; Yan, W. F.; Liang, C. D.; Dai, S. *J. Am. Chem. Soc.* **2004**, *126*, 12782.

(10) Li, Z. J.; Dai, S. *Chem. Mater.* **2005**, *17*, 1717.

(11) Chamssedine, F.; Dubois, M.; Guerin, K.; Giraudet, J.; Masin, F.; Ivanov, D. A.; Vidal, L.; Yazami, R.; Hamwi, A. *Chem. Mater.* **2007**, *19*, 161.

(12) Yang, C. M.; An, K. H.; Park, J. S.; Park, K. A.; Lim, S. C.; Cho, S. H.; Lee, Y. S.; Park, W.; Park, C. Y.; Lee, Y. H. *Phys. Rev. B* **2006**, *73*, 075419.

(13) Nakajima, T.; Matsuo, Y.; Kasamatsu, S.; Nakanishi, K. *Carbon* **1994**, *32*, 1177.

10.1021/cm071490y CCC: $40.75

postsynthesis is considerably difficult. In situ polymerization inside the channels could produce polymer modified mesoporous carbons.[34] Diazonium compound and fluorine gas were found to react with mesoporous carbon and be covalently grafted on carbon.[9,35,36] Nonuniform modification and pore blockage may be the serious problems for the postsynthesis grafting. Rigorous conditions may destroy the mesostructure to some extent. An extra step for the synthesis of mesoporous carbon is also necessary which is fabricated by using mesoporous silica as a scaffold. The multistep operation is time-consuming, and a careful control in each step is required.

A block-copolymer self-assembly approach to prepare ordered mesoporous carbon frameworks has been recently reported by several groups.[37–40] For example, Meng et al. demonstrated a reproducible synthesis of highly ordered mesoporous polymers and carbons from an organic–organic assembly of phenol, formaldehyde, and commercial PEO–PPO–PEO copolymers.[39] A family of highly ordered mesoporous polymer resins and carbons has been synthesized, including mesostructures with lamellar, 2D hexagonal $p6mm$ (FDU-15), bicontinuous cubic $Ia\bar{3}d$ (FDU-14), body-centered cubic $Im\bar{3}m$ (FDU-16), and face-centered cubic $Fd\bar{3}m$ (FDU-17) and $Fm\bar{3}m$ (FDU-18) symmetries.[41–43] Up to now, the functionalization of this kind of ordered mesoporous carbon frameworks has not been reported. The high-temperature carbonization can also eliminate the functional groups and weak C–X bonds.

In this paper, we report, for the first time, the synthesis of highly ordered fluorinated mesoporous carbons by the direct triblock-copolymer-templating approach. The organic precursors are phenol, formaldehyde, and *p*-fluorophenol. *p*-Fluorophenol serves as a functional monomer in the modification of carbon products similar to the organic group containing alkoxysilanes in the synthesis of functionalized mesoporous silicates. Triblock copolymer F127 is selected as the structure-directing agent. Highly ordered F-containing mesostructured polymer is the product from the evaporation-induced triblock-copolymer self-assembly when the ratio of *p*-fluorophenol/total phenol in the organic precursors ranges from 0 to 83%. After high-temperature carbonization at 900 °C, highly ordered mesoporous carbon with covalent C–F bonds can be obtained. The fluorinated carbon products have high surface areas and narrow pore sizes. Various mesostructures such as two-dimensional (2D) hexagonal and three-dimensional (3D) body-centered cubic structures can be synthesized by simply tuning the ratios of *p*-fluorophenol/phenol or resol/triblock copolymer. The preliminary application in electron transfer kinetics indicates that fluorinated mesoporous carbons have high redox ability.

2. Experimental Section

2.1. Chemicals. Poly(propylene oxide)–*block*–poly(ethylene oxide)–*block*–poly(propylene oxide) triblock copolymer Pluronic F127 ($EO_{106}PO_{70}EO_{106}$, $M_w = 12, 600$) and *p*-fluorophenol (99%) were purchased from Acros Chemical Inc. Phenol (C_6H_5OH, 99.98%), formalin (HCHO, 37.0–40.0%), hydrogen chloride (HCl, 36.0–38.0%), sodium hydroxide (NaOH, minimum 96.0%), and ethanol (C_2H_5OH, minimum 99.7%) were obtained from Shanghai Chemical Company. All chemicals were used as received without any further purification. Water used in all syntheses was distilled and deionized.

2.2. Synthesis of Fluororesol. In a typical preparation, 1.0 g of *p*-fluorophenol and 7.2 g of phenol were melted at 40–42 °C in a flask. To it, 1.7 g of 20 wt % NaOH aqueous solution was poured under stirring. The solution was then mixed well with 14.2 g of formalin (37 wt % formaldehyde) solution and was heated to 70–75 °C with refluxing. After 1 h, the mixture was cooled down to room temperature. A 2 M HCl solution was then added to decrease the pH to about 7.0. Water in the solution was removed by vacuum evaporation below 50 °C. The products were dissolved in ethanol to obtain a solution (20 wt %). By fixing the molar ratios of 1.0(x% *p*-fluorophenol + $(1 - x)$% phenol):2.0 formaldehyde:0.1 NaOH:6.7 H_2O and adjusting the ratios (x%) of *p*-fluorophenol, a series of fluororesols (F-resol-x) could be prepared, x ranging from 0 to 83. For example, F-resol-67 denoted the resol prepared from an

---

(14) Ryoo, R.; Joo, S. H.; Kim, J. M. *J. Phys. Chem. B* **1999**, *103*, 7435.
(15) Jun, S.; Joo, S. H.; Ryoo, R.; Kruk, M.; Jaroniec, M.; Liu, Z.; Ohsuna, T.; Terasaki, O. *J. Am. Chem. Soc.* **2000**, *122*, 10712.
(16) Lu, A. H.; Schuth, F. *Adv. Mater.* **2006**, *18*, 1793.
(17) Lu, A. H.; Li, W. C.; Schmidt, W.; Schuth, F. *Microporous Mesoporous Mater.* **2005**, *80*, 117.
(18) Yoon, S. B.; Kim, J. Y.; Yu, J. S.; Gierszal, K. P.; Jaroniec, M. *Ind. Eng. Chem. Res.* **2005**, *44*, 4316.
(19) Li, H. C.; Sakamoto, Y.; Li, Y. S.; Terasaki, O.; Thommes, M.; Che, S. A. *Microporous Mesoporous Mater.* **2006**, *95*, 193.
(20) Kruk, M.; Jaroniec, M.; Kim, T. W.; Ryoo, R. *Chem. Mater.* **2003**, *15*, 2815.
(21) Gierszal, K. P.; Jaroniec, M. *J. Am. Chem. Soc.* **2006**, *128*, 10026.
(22) Yang, H. F.; Yan, Y.; Liu, Y.; Zhang, F. Q.; Zhang, R. Y.; Meng, Y.; Li, M.; Xie, S. H.; Tu, B.; Zhao, D. Y. *J. Phys. Chem. B* **2004**, *108*, 17320.
(23) Yang, H. F.; Shi, Q. H.; Liu, X. Y.; Xie, S. H.; Jiang, D. C.; Zhang, F. Q.; Yu, C. Z.; Tu, B.; Zhao, D. Y. *Chem. Commun.* **2002**, 2842.
(24) Lee, J.; Kim, J.; Hyeon, T. *Adv. Mater.* **2006**, *18*, 2073.
(25) Lee, J.; Han, S.; Hyeon, T. *J. Mater. Chem.* **2004**, *14*, 478.
(26) Lee, J.; Kim, J.; Hyeon, T. *Chem. Commun.* **2003**, 1138.
(27) Vinu, A.; Ariga, K.; Mori, T.; Nakanishi, T.; Hishita, S.; Golberg, D.; Bando, Y. *Adv. Mater.* **2005**, *17*, 1648.
(28) Alemany, L. B.; Zhang, L.; Zeng, L. L.; Edwards, C. L.; Barron, A. R. *Chem. Mater.* **2007**, *19*, 735.
(29) Delabarre, C.; Dubois, M.; Giraudet, J.; Guerin, K.; Hamwi, A. *Carbon* **2006**, *44*, 2543.
(30) Giraudet, J.; Dubois, M.; Guerin, K.; Pinheiro, J. P.; Hamwi, A.; Stone, W. E. E.; Pirotte, P.; Masin, F. *J. Solid State Chem.* **2005**, *178*, 1262.
(31) Ning, Z. Y.; Cheng, S. H.; Chen, L. L. *Mater. Sci. Semicond. Process* **2005**, *8*, 467.
(32) Guerin, K.; Pinheiro, J. P.; Dubois, M.; Fawal, Z.; Masin, F.; Yazami, R.; Hamwi, A. *Chem. Mater.* **2004**, *16*, 1786.
(33) Chen, L. L.; Cheng, S. H.; Yu, X.; Ning, Z. Y.; Xu, S. H.; Jun, C. *Plasma Sci. Technol.* **2003**, *5*, 1977.
(34) Choi, M.; Kleitz, F.; Liu, D. N.; Lee, H. Y.; Ahn, W. S.; Ryoo, R. *J. Am. Chem. Soc.* **2005**, *127*, 1924.
(35) Toupin, M.; Belanger, D. *J. Phys. Chem. C* **2007**, *111*, 5394.
(36) Vase, K. H.; Holm, A. H.; Norrman, K.; Pedersen, S. U.; Daasbjerg, K. *Langmuir* **2007**, *23*, 3786.
(37) Tanaka, S.; Nishiyama, N.; Egashira, Y.; Ueyama, K. *Chem. Commun.* **2005**, 2125.
(38) Liang, C. D.; Dai, S. *J. Am. Chem. Soc.* **2006**, *128*, 5316.
(39) Meng, Y.; Gu, D.; Zhang, F. Q.; Shi, Y. F.; Yang, H. F.; Li, Z.; Yu, C. Z.; Tu, B.; Zhao, D. Y. *Angew. Chem., Int. Ed.* **2005**, *44*, 7053.
(40) Zhang, F. Q.; Meng, Y.; Gu, D.; Yan, Y.; Yu, C. Z.; Tu, B.; Zhao, D. Y. *J. Am. Chem. Soc.* **2005**, *127*, 13508.
(41) Meng, Y.; Gu, D.; Zhang, F. Q.; Shi, Y. F.; Cheng, L.; Feng, D.; Wu, Z. X.; Chen, Z. X.; Wan, Y.; Stein, A.; Zhao, D. Y. *Chem. Mater.* **2006**, *18*, 4447.
(42) Deng, Y. H.; Yu, T.; Wan, Y.; Shi, Y. F.; Meng, Y.; Gu, D.; Zhang, L. J.; Huang, Y.; Liu, C.; Wu, X. J.; Zhao, D. Y. *J. Am. Chem. Soc.* **2007**, *129*, 1690.
(43) Huang, Y.; Cai, H. Q.; Yu, T.; Zhang, F. Q.; Zhang, F.; Meng, Y.; Gu, D.; Wan, Y.; Sun, X. L.; Tu, B.; Zhao, D. Y. *Angew. Chem., Int. Ed.* **2007**, *46*, 1089.

initial mixture with 67% *p*-fluorophenol and 33% phenol in molar ratio.

2.3. Synthesis of Fluorinated Mesoporous Carbons. Fluorinated mesoporous carbons were prepared by coassembly of fluororesols and triblock copolymer F127 via the evaporation-induced self-assembly (EISA) strategy. The synthesis was similar to the established procedure, except that the F-resol-*x* ethanolic solution instead of resol was used. The synthesis compositions (molar ratios) for the 2D hexagonal mesostructure were in the range of *p*-fluorophenol:phenol:formaldehyde:NaOH:F127 = 0.1:0.9:2: 0.1:0.009–0.0065, 0.5:0.5:2:0.1:0.0051–0.0055, or 0.67:0.33:2:0.1: 0.0040–0.0044, and for the 3D body-centered cubic mesostructure, they were in the range of 0.1:0.9:2:0.1:0.0033–0.0061, 0.5:0.5:2: 0.1:0.0033–0.0049, or 0.67:0.33:2:0.1:0.0033–0.0037. In a detailed procedure, to a clear solution with 0.80 g of triblock copolymer F127 and 16.00 g of ethanol, 8.00 g of 20 wt % F-resol-10 ethanolic solution was added. The mixture was stirred for 10 min and then transferred into dishes. It took 5–8 h to evaporate ethanol at room temperature. Thermopolymerization of the polymer precursors was carried out at 100 °C for 24 h in an oven. Products were collected by scraping from the dishes and put in a tubular furnace. The heating temperature, time, and atmosphere were 900 °C, 4 h, and nitrogen, respectively. Mesoporous carbon product was obtained and named as F-FDU15-10. The names of mesoporous carbons (FDU-15 and FDU-16) come from the literature which represent highly ordered mesoporous carbons with the 2D hexagonal (space group *p*6*mm*) and the 3D body-centered cubic structures (space group $Im\bar{3}m$), respectively. The last number in the name represents *x* in the initial organic precursor F-resol-*x*.

2.4. Characterization. The small-angle X-ray scattering (SAXS) measurements were taken on a Nanostar U small-angle X-ray scattering system (Bruker) using Cu Kα radiation (40 kV, 35 mA). The *d* spacing values were calculated by the formula $d = 2\pi/q$, and the unit cell parameters were calculated from the formula $a = 2d_{100}/\sqrt{3}$ and $a = \sqrt{2}d_{110}$ for F-FDU15 and F-FDU16, respectively. N_2 adsorption–desorption isotherms were measured at 77 K with a Quantachrome NOVA 4000e analyzer. The Brunauer–Emmett–Teller (BET) method was utilized to calculate the specific surface areas (S_{BET}). By using the Barett–Joyner–Halenda (BJH) model, the pore volumes and pore size distributions were derived from the adsorption branches of isotherms, and the total pore volumes (V_t) were estimated from the adsorbed amount at a relative pressure p/p_0 of 0.99. The micropore volume (V_m) and micropore surface area were calculated from the *V*–*t* plot method. The *t* values were calculated as a function of the relative pressure using the de Boer equation, $t/\text{Å} = [13.99/(\log(p_0/p) + 0.0340)]^{1/2}$. V_m was obtained using the equation $V_m/\text{cm}^3 = 0.001547I$, where *I* represents the *Y* intercept in the *V*–*t* plot. Transmission electron microscopy (TEM) experiments were conduced on a JEOL 2011 microscope operated at 200 kV. The samples for TEM measurements were suspended in ethanol and supported onto a holey carbon film on a Cu grid. Fourier transform infrared (FTIR) spectra were collected on Nicolet Fourier spectrophotometer, using KBr pellets of the solid samples. Wide-angle X-ray diffraction (XRD) measurements were performed on a Rigaku Dmax-3C diffractometer with Cu Kα radiation (40 mV, 40 mA). Raman spectra were obtained with a Super LabRam microscopic Raman spectrometer, using a He–Ne laser with an excitation wavelength of 633 nm. ^{13}C NMR (nuclear magnetic resonance) spectra were collected at room temperature with a frequency of 75 MHz (2 s recycle, 2.5 ms contact time) using adamantane as a reference.

2.5. Electrochemical measurements. Cyclic voltammetry measurements were performed on a CHI660 electrochemical workstation with a conventional three-electrode cell. A glassy carbon (GC) electrode, platinum electrode, and saturated calomel electrode (SCE) were used as the working electrode, counter electrode, and reference electrode, respectively. The GC electrode (3 mm in diameter) was polished to a mirrorlike surface with 1.0, 0.30, and 0.050 mL alumina slurry followed by rinsing thoroughly with water. The electrodes were successively sonicated in 1:1 nitric acid, acetone, and doubly distilled water and then allowed to dry at room temperature. A 20 μL portion of 2.6 mg/mL mesoporous carbon in *N*, *N*-dimethyl formamide (DMF) suspension was dropped on the surface of a pretreated GC electrode and dried under an infrared lamp to obtain the ordered mesoporous carbon modified GC electrode. All experimental solutions were deoxygenated by bubbling high-purity nitrogen for at least 15 min and maintained under nitrogen atmosphere during measurement. Experiments were carried out at room temperature.

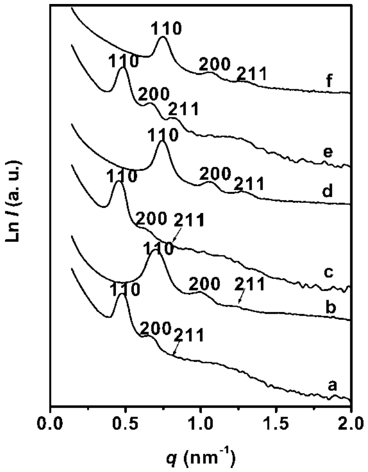

Figure 1. SAXS patterns of mesoporous materials synthesized by using F-resols as organic precursors and triblock copolymer as a template via the EISA method: as-made materials F-FDU16-67 (a), F-FDU16-50 (c), and F-FDU16-10 (e) and carbons calcined at 900 °C under nitrogen F-FDU16-67 (b), F-FDU16-50 (d), and F-FDU16-10 (f).

3. Results and Discussion

Fluorinated mesoporous carbon materials were prepared by the coassembly of triblock copolymer F127 and F-resol via the EISA approach. Beginning with 15.0 g of F-resol-67, which contains 6.4 g of *p*-fluorophenol, 2.6 g of phenol, 14.2 g of formaldehyde, and 3.8 g of triblock copolymer F127, the as-made membranes are transparent and soft (as shown by the image Figure 1 in the Supporting Information), indicating no macrophase separation. The SAXS pattern of as-made F-FDU16-67 shows an intense diffraction peak and two weak peaks at *q* values of 0.5, 0.7, and 0.82 nm^{-1} that can be indexed as 110, 200, and 211 reflections of the 3D body-centered cubic mesostructure with the $Im\bar{3}m$ symmetry (Figure 1). Upon calcination at 900 °C under nitrogen, the three-peak SAXS pattern can be clearly observed, indicating that the cubic mesostructure is stable. The cell parameter before and after heating is calculated to be 18.5 and 12.6 nm, respectively, indicative of a large structural shrinkage of 32%. This value is close to the pure carbon FDU-16, suggesting a minor effect of the F incorporation on the mesostructure. TEM images (Figure 2) for fluorinated carbon F-FDU16-67 display typical patterns of a body-centered cubic structure viewed along the [110], [100], and [111] directions, confirming the highly ordered mesostructure. The

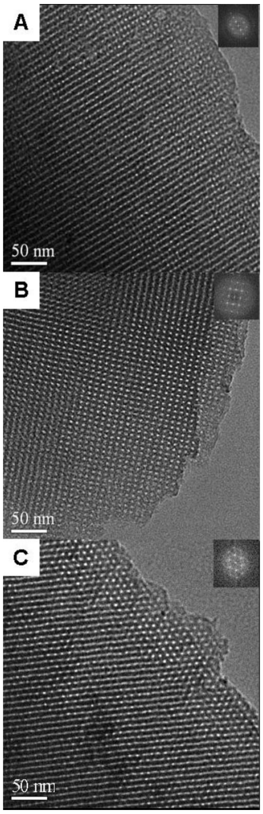

Figure 2. TEM images of F-FDU16-67 viewed from the (A) [110], (B) [100], and (C) [111] directions prepared by the direct triblock-copolymer-templating approach. The insets are corresponding fast Fourier transform (FFT) diffractograms.

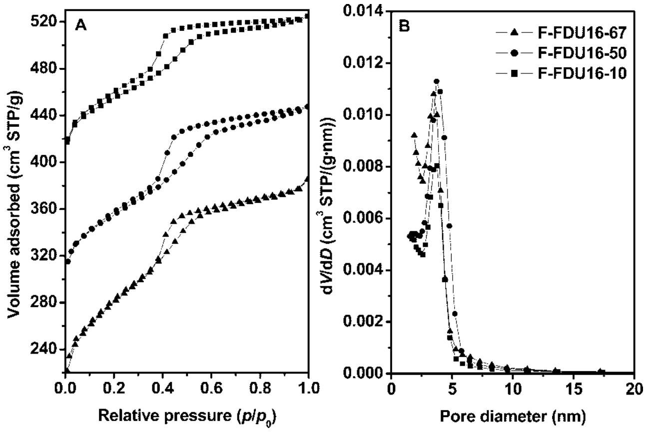

Figure 3. (A) Nitrogen sorption isotherms and (B) pore size distribution curves of F-FDU16-67, F-FDU16-50, and F-FDU16-10 carbon materials. The isotherms for F-FDU16-50 and F-FDU16-10 are offset vertically by 120 and 240 cm^3/g, respectively.

cell parameter is estimated to be 12.0 nm, in good agreement with that from the SAXS pattern. By using F-resols prepared from the mixtures with the percentage of *p*-flurophenol ranging from 0 to 50% as precursors and tuning the amount of triblock copolymer F127, the SAXS patterns of the as-made materials (F-FDU16-10 and F-FDU16-50) also exhibit characteristic scattering peaks of the ordered body-centered cubic mesostructure (Figure 1). After heating at 900 °C in the inert atmosphere, the SAXS patterns get more resolved, indicating that the cubic mesostructures are highly stable, in accordance with the above results.

Table 1. Structural and Textual Properties of Pure and Fluorinated Mesoporous Carbons

sample	unit cell parameter a_0 (nm)	BET surface area (m^2/g)	micropore surface area (m^2/g)	pore size (nm)	pore volume (cm^3/g)	micropore volume (cm^3/g)
F-FDU16-67	12.6	944	790	3.5	0.60	0.24
F-FDU16-50	11.9	741	602	3.7	0.49	0.21
F-FDU16-10	11.9	715	611	3.6	0.43	0.21
FDU-16	13.1	812	663	4.0	0.44	0.23
F-FDU15-67	9.6	693	577	3.0	0.43	0.18
F-FDU15-50	10.2	792	625	3.7	0.53	0.21
F-FDU15-10	11.2	998	757	4.4	0.70	0.27
FDU-15	11.4	875	683	4.0	0.59	0.24

Nitrogen sorption isotherms of the above three F-FDU16 samples (Figure 3A) show typical type-IV curves with a sharp capillary condensation step at middle relative pressures of 0.35–0.65, corresponding to the narrow pore size distribution (Figure 3B). The BET surface areas, total pore volumes, and pore sizes are about 750 m^2/g, 0.45 cm^3/g, and 3.5 nm (Table 1), respectively, which are analogous to the pure carbon framework FDU-16. A distinct phenomenon in Figure 3B is the presence of micropores. Indeed, the micropores contribute to a large extent to the BET surface areas and the pore volumes, in coincidence with that for pure mesoporous carbon FDU-16. These results reveal that the fluorine-functionalized mesoporous carbon materials can maintain the topologies upon high-temperature carbonization. The F content in the synthesis exhibits slight influence on the mesostructure.

When the initial mass ratio of F-resol to triblock copolymer F127 decreases, transparent membranes without macrophase separation can also be obtained (images not shown). The as-made F-FDU15-10, F-FDU15-50, and F-FDU15-67 products display well-resolved SAXS patterns with at least three reflections at *q* values ranging from 0.45 to 1.14 nm^{-1}, associated with the highly ordered 2D hexagonal mesostructure (Figure 4). After carbonization at 900 °C, the SAXS peaks are reserved, appearing at slightly larger *q* values. These results indicate the stable hexagonal mesostructure with the shrinkage in the domain size of about 25%. TEM images of F-FDU15-50 after calcination at 900 °C (Figure

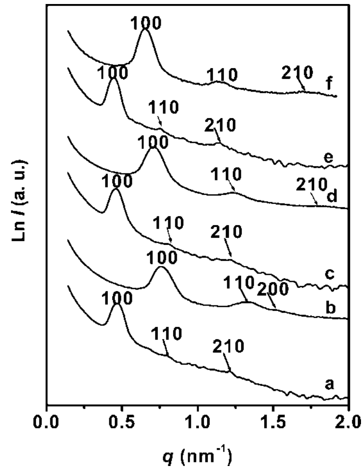

Figure 4. SAXS patterns of fluorinated mesoporous carbons which were prepared from a solution containing different percentages of *p*-fluorophenol: as-made materials F-FDU15-67 (a), F-FDU15-50 (c) and F-FDU15-10 (e) and carbons after calcination at 900 °C under nitrogen F-FDU15-67 (b), F-FDU15-50 (d), and F-FDU15-10 (f).

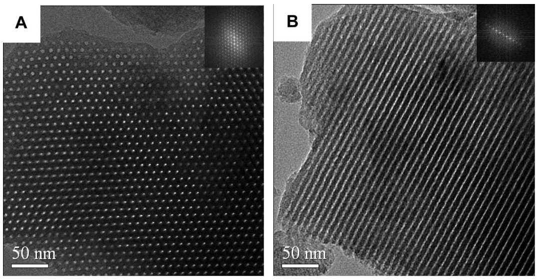

Figure 5. TEM images of fluorinated mesoporous carbon F-FDU15-50 prepared by using F-resol-50 as an organic precursor and triblock copolymer F127 as a template via the EISA method after carbonization at 900 °C under nitrogen atmosphere, viewed from the (A) [001] and (B) [110] directions. The insets are corresponding FFT diffratograms.

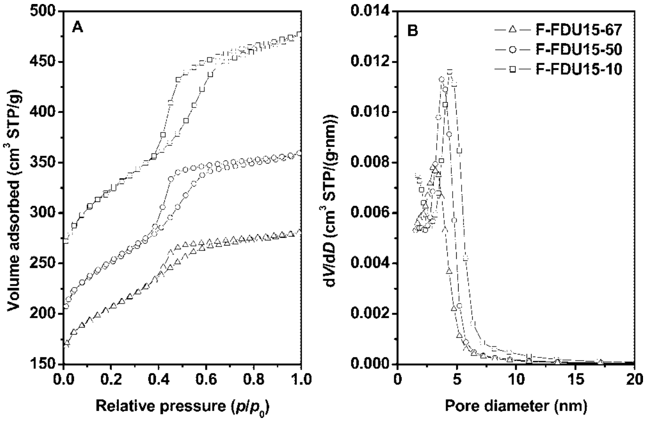

Figure 6. (A) Nitrogen sorption isotherms and (B) pore size distribution curves of fluorinated mesoporous carbons after calcination at 900 °C under nitrogen atmosphere.

5) show well-ordered arrays in large domains, further confirming an ordered 2D hexagonal mesostructure with 1D channels. The cell parameter (a_0) estimated from the TEM images is approximately 11.0 nm, in accordance with the value calculated from the SAXS data. Typical type-IV isotherms with sharp capillary condensation steps at middle relative pressures of 0.40–0.70 are observed for all three samples (Figure 6). The sharp step reflects a narrow pore size distribution. F-FDU15 materials have the pore sizes of 3.0–4.0 nm, BET surface areas of 693–998 m^2/g, and pore volumes of 0.43–0.70 cm^3/g (Table 1). Similar to F-FDU16s, the BET surface areas and the pore volumes are principally resulted from the micropores.

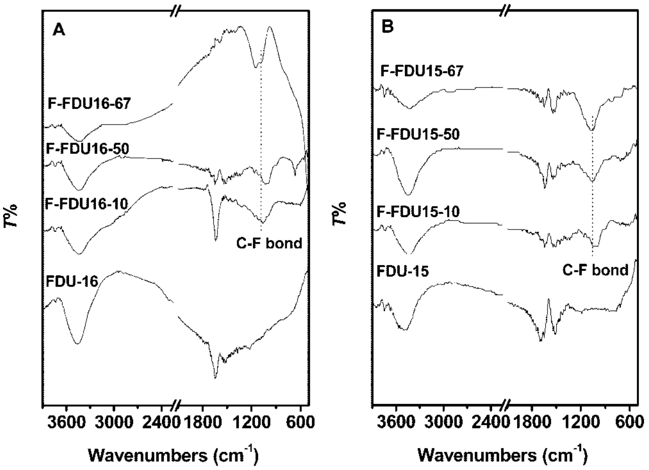

Figure 7. FTIR spectra of pure and fluorinated mesoporous carbons after high-temperature (900 °C) carbonization with (A) the 3D body-centered cubic and (B) the 2D hexagonal mesostructures.

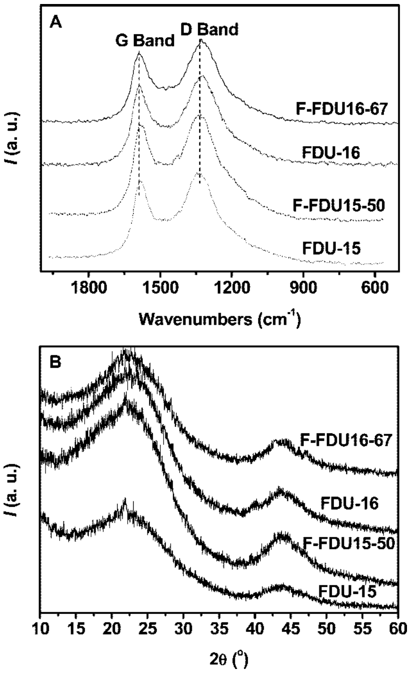

Figure 8. (A) Raman spectra and (B) wide-angle XRD patterns of pure and fluorinated mesoporous carbons heated at 900 °C in nitrogen atmosphere.

FTIR spectra of the fluorine-functionalized and pure mesoporous carbon materials after carbonization at 900 °C for 4 h in N_2 atmosphere are shown in Figure 7. The spectra of mesoporous carbons (both FDU-16 and FDU-15) exhibit no obvious vibrations similarly to the previous report, which is the character of pure carbon materials.[41] Fluorine-containing mesoporous carbons display the similar FTIR spectra to pure mesoporous carbons. The only difference is a band at 1030–1130 cm^{-1}, which can be assigned to the covalent C–F stretching vibration.[44] The results clearly indicate that fluorine-functionalized mesoporous carbons have the carbon frameworks with the C–F covalent bonds. With the increase of F content in the initial material, the relative intensity of C–F vibration increases. Raman spectra of the pure and fluorinated mesoporous carbon materials (F-FDU16-67 and F-FDU15-50) carbonized at 900 °C in N_2 atmosphere are given in Figure 8A. A distinct pair of broad bands at 1590 cm^{-1} (G band) and 1321 cm^{-1} (D band) can be observed. The ratio of I_D/I_G slightly increases after the incorporation of fluorine in mesoporous carbons. This suggests the carbon framework of F-FDU16-67 and the modification by fluorine. Wide-angle XRD patterns (Figure 8B) of FDU-16 and F-FDU16-67 exhibit two broad diffraction peaks at 2θ of about 22 and 44°, corresponding to 002 and 01 diffractions of amorphous carbon, respectively.

These results suggest that hybrid fluorinated mesoporous carbons can be prepared from the direct triblock-copolymer-templating EISA approach. This process undergoes several steps. The first one is the co-condensation of *p*-fluorophenol,

---

(44) Dyer, R. J. *Applications of absorption spectroscopy of organic compounds*; Prentice Hall of India: New Delhi, 1974.

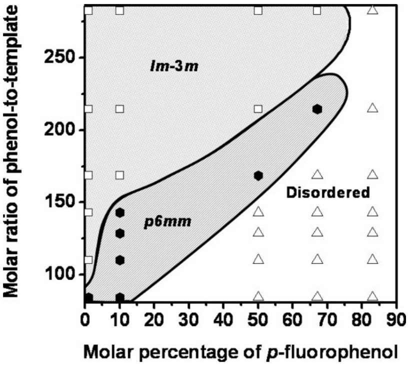

Figure 9. Synthetic space diagram of mesostructures established according to SAXS measurements.

phenol, and formaldehyde to form F-resols. Second, the self-assembly of triblock copolymer F127 with F-resols occurs during the evaporation of ethanol. Then, the thermopolymerization of phenolic resins is proceeded to solidify the F-phenolic resin/triblock copolymer nanocomposites. The following calcination at low temperature (350 °C) and carbonization at high temperature (900 °C) leads to the elimination of triblock copolymer and the formation of fluorine-containing carbons.

The synthesis of organic precursor F-resol is the key step. F-resol is prepared by the copolymerization of *p*-fluorophenol, phenol, and formaldehyde under basic conditions, which is water- and ethanol-soluble. Precipitation would occur when *p*-fluorophenol reacts with formaldehyde under the same conditions. The ^{13}C NMR spectra of the resultants and pure resols are shown in Figure 2 of the Supporting Information. The carbon atoms in the resol-type resins are extremely complicated. No standard spectra can be found in the references due to the variation in the molecular weight. F-resols display the similar ^{13}C NMR spectra to resols. The tri- or tetrasubstituted benzene rings, phenolic hydroxyl groups, and benzyl hydroxyl groups can be detected. These results possibly indicate that *p*-fluorophenol participates in the condensation with formaldehyde, similar to phenol. In addition, the molar ratio of the benzyl hydroxyl groups to phenol declines from 30.4, 24.7, and 19.0 to 14.1% when the initial molar ratio of *p*-fluorophenol in the total phenols rises from 0, 10, and 50 to 67%. *para*-Substituted fluorine may occupy one active site for the condensation of phenolic aldehyde, possibly inhibiting the reaction. These results give evidence on the incorporation of fluorine into resol networks. The C–F covalent bonds can be retained even after high-temperature carbonization under N_2 atmosphere owing to the high energy.[45]

The relationship among the molar ratios of the phenols to triblock copolymer F127 and *p*-fluorophenol to phenol and the final mesostructure are shown in Figure 9. It can be clearly concluded that the molar ratio ranges for the formation of the $Im\bar{3}m$ and the *p6mm* mesostructures are relatively wide and both the ratios of phenol/F127 and *p*-fluorophenol/phenol influence the final mesostructures. For example, 2D hexagonal F-FDU15-10 can be synthesized with the molar ratio of phenol/F127 ranging from 70 to 140. Further increasing this ratio leads to the formation of the 3D cubic F-FDU16-10 mesostructure. Similar to the resols,[39,41,43] the F-resol precursor can incorporate with the PEO blocks of the copolymer via the strong H-bonds. The increase of the phenol/F127 ratio results in the increase of hydroxyl groups including phenolic and benzyl hydroxyl groups, the swelling of the hydrophilic volume with the maintenance of the hydrophobic volume per block, and, in turn, a curvature at the PEO/PPO interface.[46–48] Therefore, the increase of hydrophilic/hydrophobic ratio in the triblock-copolymer–resol composite causes the mesophase transformation from the 2D hexagonal to the 3D body-centered cubic mesostructure.

On the other hand, the range of phenol/F127 for the synthesis of FDU-16 is about 100–280, while F-FDU16-67 can only be obtained at the phenol/F127 ratio of 280. The corresponding range of this molar ratio is 210–280 and 170–280 if the molar percentage of *p*-fluorophenol reduces to 50 and 10% in the initial mixture, respectively. This reflects the fact that, to synthesize a given highly ordered mesostructure, the required amount of the organic precursor enlarges with the increase of the molar percentage of *p*-fluorophenol. This phenomenon may be related to the decrease of hydroxyl groups in the F-resols prepared from a large amount of *p*-fluorophenol. Moreover, the inherent hydrophobicity of C–F may reduce the hydrophilic/hydrophobic ratio of the triblock-copolymer–resol composites. The higher percentage of *p*-fluorophenol is, the more the required amount of F-resol is. The highly ordered mesostructure cannot be formed if the molar content of *p*-fluorophenol in the total phenol exceeds 83%. The lack of the hydroxyl groups and the increase of hydrophobicity may lead to the failing assembly of F-resols prepared from a high molar percentage of *p*-fluorophenol and the amphiphilic triblock copolymer.

The content of *p*-fluorophenol in the synthesis shows a minor effect on the structural regularity. This phenomenon is dissimilar to the fluorination on mesoporous carbons with fluorine gas.[9] The fluorination between the fluorine gas and the mesoporous carbon replicas results in a gradual structural degradation due to the formation of sp^3-hydridized carbon. In the present case, however, the covalent C–F bonds have existed from the beginning and are maintained during the assembly, thermopolymerization, and high-temperature carbonization. The effect of C–F bonds on the ordering of the mesostructure may be neglected once the highly ordered mesostructure is formed.

3.1. Study on Electron Transfer Kinetics. Fluorinated ordered mesoporous carbon products were examined by performing cyclic voltammetry with the model redox couple $Fe(CN)_6^{4-}/Fe(CN)_6^{3-}$ to evaluate the electron-transfer properties. Figure 10A plots the cyclic voltammograms obtained at the F-FDU15-50 modified GC electrode in the presence of 5 mM $K_4Fe(CN)_6$ in 0.1 M KCl with different scan rates.

---

(45) Kazanjian, A. R.; Horrell, D. R. *J. Phys. Chem.* **1971**, *75*, 2217.

(46) Liu, X. Y.; Tian, B. Z.; Yu, C. Z.; Gao, F.; Xie, S. H.; Tu, B.; Che, R. C.; Peng, L. M.; Zhao, D. Y. *Angew. Chem., Int. Ed.* **2002**, *41*, 3876.

(47) Wan, Y.; Shi, Y. F.; Zhao, D. Y. *Chem. Commun.* **2007**, 897.

(48) Wan, Y.; Zhao, D. Y. *Chem. Rev.* **2007**, *107*, 2821.

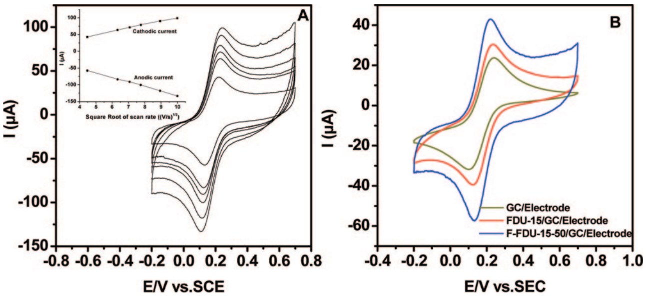

Figure 10. (A) Cyclic voltammograms of ordered mesoporous carbon containing the F-FDU15-50 modified electrode in 5 mM $K_4Fe(CN)_6$ in 0.1 M KCl solution at different scan rates. The scan rates were as follows (from inner to outer): 20, 40, 50, 60, 80, and 100 mV/s. The inset is the plots of peak current vs the square root of the scan rate. (B) Cyclic voltammograms of bare electrode and modified electrodes in 5 mM $K_4Fe(CN)_6$/0.1 M KCl solution at 20 mV/s.

The symmetrical shape of the redox peaks can be observed in the potential range between −0.2 and 0.7 V. The peak-to-peak separation (ΔE_p) expands, and the redox peak currents linearly increase with the increase of the scan rate in the experimental range. These phenomena suggest the quasireversible behavior and linear diffusion conditions.[49,50]

The cyclic voltammograms obtained at the F-FDU15-50 modified, pure carbon FDU-15 modified, and bare GC electrode in the presence of 5 mM $K_4Fe(CN)_6$ in 0.1 M KCl at 20 mV/s are displayed in Figure 10B. The peak-to-peak separation is 87 mV for the F-FDU15-50 modified electrode, 107 mV for the FDU-15 modified GC electrode, and 138 mV for the bare GC electrode. The ΔE_p value is the difference in the potential between the anodic and cathodic peaks, associated to the rate of electron transfer. A lower ΔE_p corresponds to a higher electron transfer rate. It is therefore the electron transfer rates are in the sequence of F-FDU15-50 modified GC > FDU-15 modified GC > bare GC electrode. The electron transfer rate constant k_0, estimated from the Nicholson's method, is 0.005, 0.0025, and 0.0013 cm/s for the F-FDU15-50 modified, FDU-15 modified, and bare GC electrodes, respectively.

The electrochemical behaviors can be influenced by the graphitic nature and the structural and chemical properties of the electrodes.[51–53] The reduction of I_D/I_G in the Raman spectrum is related to the increase of the graphitic degree. All these three electrodes show weak graphitic nature (Figure 8 and Figure 3 in the Supporting Information). As a consequence, the different behaviors in the electrochemical properties of F-FDU15-50 modified, FDU-15 modified, and bare GC are possibly attributed to the structural and chemical modification. The ordered 2D hexagonal mesoporous carbon FDU-15 greatly enhances the electrochemical properties and exhibits a fast electron transfer rate. These properties can be further improved by the fluorine-incorporated ordered mesoporous carbon, which gives further evidence on the incorporation of fluorine on mesoporous carbon. The reasonably high redox ability may be attributed to the integrity of the carbon framework,[51] large pore sizes of FDU-15 and F-FDU15-50, and, more importantly, fluoro-functionalization on F-FDU15-50. The electrochemically reductive properties of hybrid C–F bonds may enhance the electron transfer rate.

4. Conclusions

A direct triblock-copolymer-templating approach is demonstrated for the successful synthesis of ordered mesoporous carbons containing fluorine. The organic precursors are phenol, formaldehyde, and a functional monomer *p*-fluorophenol which can polymerize to generate soluble phenolic resins modified with fluorine. During the EISA process, the assembly of these F-resols with triblock copolymer F127 can proceed when the ratio of *p*-fluorophenol/total phenol in the organic precursors does not exceed 83%. After high-temperature carbonization at 900 °C, the mesoporous carbon products have highly ordered mesostructures (2D hexagonal and 3D body-centered cubic), high surface areas (693–998 m^2/g), uniform and large pore sizes (3.0–4.4 nm), large pore volumes (0.43–0.70 cm^3/g), and C–F covalent bonds that can be preserved. The mesostructures can be tuned by simply adjusting the ratios of *p*-fluorophenol/phenol or F-resol/triblock copolymer. These values affect the amounts of hydroxyl groups in organic precursors, tune the hydrophilic/hydrophobic ratios of the resol–triblock-copolymer composites, and, in turn, change the surface curvatures. The fluorine functionalized mesoporous carbon modified electrode exhibits a higher electron transfer rate than both pure mesoporous carbon FDU-15 modified and bare GC electrodes, further suggesting the incorporation of fluorine on mesoporous carbon and showing potentials in electrocatalytic reactions.

Acknowledgment. This work was supported by the NSF of China (20407014 and 20521140450), Shanghai Sci. & Tech., Edu. Committee (07QH14011, 0652nm024, and T0402), and the Program for New Century Excellent Talents in Universities.

Supporting Information Available: Photograph of the as-made membrane of F-FDU16-67, ^{13}C NMR spectra of the resol precursors and F-resols, and Raman spectrum of the GC electrode. This material is available free of charge via the Internet at http://pubs.acs.org.

CM071490Y

---

(49) Moore, R. R.; Banks, C. E.; Compton, R. G. *Anal. Chem.* **2004**, *76*, 2677.
(50) Gavalas, V. G.; Andrews, R.; Bhattacharyya, D.; Bachas, L. G. *Nano Lett.* **2001**, *1*, 719.
(51) Lee, K. T.; Lytle, J. C.; Ergang, N. S.; Oh, S. M.; Stein, A. *Adv. Funct. Mater.* **2005**, *15*, 547.
(52) Banks, C. E.; Crossley, A.; Salter, C.; Wilkins, S. J.; Compton, R. G. *Angew. Chem., Int. Ed.* **2006**, *45*, 2533.
(53) Moore, R. R.; Banks, C. E.; Compton, R. G. *Anal. Chem.* **2004**, *76*, 2677.